JTTEE5 19:190–197
DOI: 10.1007/s11666-009-9410-6
1059-9630/$19.00 © ASM International

Feather-like Structured YSZ Coatings at Fast Rates by Plasma Spray Physical Vapor Deposition

A. Shinozawa, K. Eguchi, M. Kambara, and T. Yoshida

(Submitted April 23, 2009; in revised form August 10, 2009)

A variety of yttria-stabilized zirconia (YSZ) coatings have been attained by plasma spray physical vapor deposition (PS-PVD) with fine YSZ powders at high power. The coating structures were found to change significantly with the powder feeding rates but less with the substrate temperature and the rate of the substrate rotation, and a porous feather like structure was attained at 500 Torr (666.6 millibar) and a rate of >200 μm/min. Such a coating produces porosity reaching >50%, thermal conductivity as small as 0.5 W/mK and lower infra-red transmittance compared to the sprayed splat coating with identical thickness.

Keywords plasma spray, porosity, thermal barrier coating, thermal conductivity, yttria-stabilized zirconia

1. Introduction

In the last decade, thermal barrier coatings (TBCs) have been developed considerably as an essential component of turbine to achieve high performance and high efficiency at elevated temperatures. Yttria-stabilized zirconia (YSZ) has been most commonly used owing to its numerous advantages such as low thermal conductivity, high melting point, chemical inertness, and compatible thermal expansion coefficient to the metallic bond coat and substrate (Ref 1). It is also well known that the thermal and mechanical properties of TBCs depend critically on the microstructure of the coatings. Therefore, numbers of study on the process development have been carried out for better control of the YSZ coating microstructure. Especially, as the thickness of the TBCs must usually be over several hundreds of microns for their practical performance, the deposition rate and cost efficiency have been the major concerns in developing the manufacturing methods. Typically, atmospheric plasma spraying (APS) and electron-beam physical vapor deposition (EB-PVD) have been employed for commercial applications. However, each of these processes has its pros and cons. APS achieves relatively low thermal conductivities owing to the unique splat-layered coating structure together with its high-speed deposition characteristics (Ref 2). In contrast, EB-PVD process is known to be superior to APS as it generally produces high strain tolerant and excellent thermal shock resistant coatings with typical columnar microstructure, although several drawbacks are recognized such as relatively high thermal conductivity and low deposition rate (Ref 3).

As a fundamental characteristics of the plasma spraying, loading of the injected powders to the plasma is known as a critically influential factor for both coating quality and process throughput due to its effect on the heating history of the powders during flight within the plasma flame. The essential role of the parameters has been well modeled in several literatures (Ref 4, 5). This, however, in turn suggests that the fundamental deposition process can be controlled to either spraying with molten droplets after complete melting, or the physical vapor deposition through complete evaporation of the injected feedstock, with an appropriate tuning of the loading effect, i.e., the plasma input power, the size of the feedstock power, and the feeding rate. In other words, it is possible to attain various coating structures via vapor phase deposition at a practically high speed. To underline these characteristics of the plasma spraying, the former can technically be called plasma powder spraying (PPS) and the latter plasma spray physical vapor deposition (PS-PVD). The maximum limit of the powder feeding rate for complete evaporation of YSZ powders has been estimated numerically and found to vary with pressure for the case of the hybrid plasma spray system (Ref 6). In fact, we have attempted PS-PVD of YSZ and produced YSZ coatings with various microstructures at ultrafast deposition rate as

This article is an invited paper selected from presentations at the 2009 International Thermal Spray Conference and has been expanded from the original presentation. It is simultaneously published in *Expanding Thermal Spray Performance to New Markets and Applications: Proceedings of the 2009 International Thermal Spray Conference*, Las Vegas, Nevada, USA, May 4-7, 2009, Basil R. Marple, Margaret M. Hyland, Yuk-Chiu Lau, Chang-Jiu Li, Rogerio S. Lima, and Ghislain Montavon, Ed., ASM International, Materials Park, OH, 2009.

A. Shinozawa, K. Eguchi, M. Kambara, and **T. Yoshida**, Department of Materials Engineering, The University of Tokyo, 7-3-1, Hongo, Bunkyo-Ku, Tokyo 113-8656, Japan. Contact e-mail: mkambara@plasma.t.u-tokyo.ac.jp.

high as 150 μm/min (Ref 7). Examples are a fairy dense coating with columnar structures similar to those deposited by EB-PVD, a feather-like microstructure, and a vapor-deposited structure mixed with solidified droplets. Uniqueness of these structures are evident from the facts that the YSZ coating attains thermal conductivity as low as 0.7 W/mK and that the interlaced structure with t-ZrO_2 (t = tetragonal) twin forms within a dense YSZ coating and affects the hardness and light reflectance in the infra-red wavelength (Ref 8, 9). In this work, we have attempted PS-PVD for control of feather-like structures and their thermal and optical properties were compared.

2. Experimental

Plasma spraying system equipped with two 150-kW hybrid plasma torches was used in this study to deposit various YSZ coatings, as shown in Fig. 1. The detailed descriptions of the hybrid plasma torch and the twin hybrid plasma spray system can be found elsewhere (Ref 7, 8, 10). In the present work, the first hybrid torch was used for deposition while the second hybrid torch was used for the plasma annealing purpose to facilitate instantaneous annealing (strengthening) during deposition.

The typical deposition conditions are summarized in Table 1. Referring to the experimental conditions in the previous work (Ref 7) for the PS-PVD, i.e., complete evaporation of the injected YSZ powders, plasma was generated with Ar-15%H_2 gas at high RF input power of 100 kW at a pressure of 500 Torr. Fine powders with average diameter of 5 to 15 μm (7wt%Y_2O_3-ZrO_2 AMPERIT® 825.09, H.C. Starck GmbH) were used throughout the experiment, and they were fed at the rates of 0.8, 1.6, and 3.2 g/min. Graphite substrates were used for deposition and placed on a revolving substrate holder,

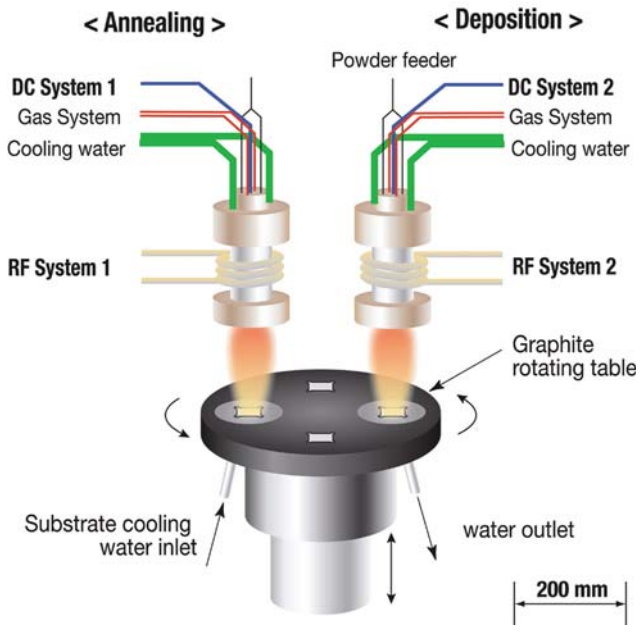

Fig. 1 Schematic illustration of the twin hybrid plasma spray system. The substrates placed on a water-cooled graphite rotation substrate holder are subject alternatively to plasma flames for deposition and annealing

Table 1 Typical experimental parameters

Parameters	Values
DC plasma, kW (deposition)	8
PR Plasma, kW (deposition)	100
DC plasma, kW (annealing)	8
RF plasma, kW (annealing)	100
Pressure, Torr	500
DC plasma gas flow rate (Ar), slm	10
RF plasma gas flow rate (Ar, H2), slm	200
Carrier gas flow rate (Ar), slm	4
Powder size, μm	5-15
Powder feeding rate, g/min	0.8-3.2
Torch-to-substrate distance, mm	25-50
Substrate revolution speed, rpm	10-50

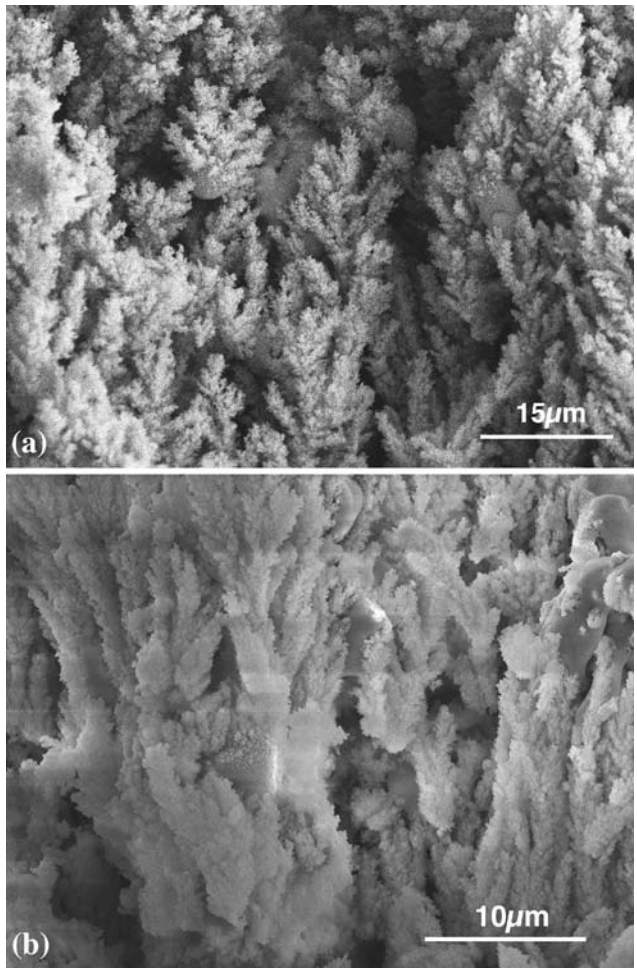

Fig. 2 The typical SEM cross-sectional image of YSZ coating, deposited by single-torch, at different torch-to-substrate distance: (a) 50 mm and (b) 25 mm

such that the substrates were exposed to the plasma flames cyclically for deposition and annealing. The substrate holder was rotated at different rates of 10, 30, and 50 rpm. The distance between the torch exit and substrate is known to affect the condensation and coagulation of the vaporized materials at the plasma and flame region above the substrate. Although the unique feather-like structure was attained at 50 mm, as shown in Fig. 2(a), these structures were not observed uniformly within the coating possibly due to various degree of collision of growth precursors in a relatively short plasma flame at high pressure. Therefore, in order to improve the uniformity of the structure over a wider area, the distance was set to 25 mm throughout the present work, producing a typical coating structure shown in Fig. 2(b). The substrate temperature was monitored at the back of the substrate through the water-cooling attachment during experiment by R-type thermocouple.

Advantages of using the graphite substrate are to withstand high temperature during deposition as well as to facilitate the microstructural observation of the coating at its cross section by simply fracturing the substrate. Additional advantage is that the YSZ coating can be separated from the graphite substrate without applying unnecessary force to break the coating structure. It was made possible by heating the coated specimen in a box furnace under ambient air up to 1200 °C for 14 h. The graphite substrate was burnt out accordingly and only the YSZ coating remained. Although high temperature annealing is considered to cause phase change and annealing, the original structure of the as-deposited coating was retained and no significant phase change was confirmed after annealing, as seen from the typical structures observed by a field-emission scanning electron microscopy (FE-SEM: S-4200, Hitachi Ltd.) and x-ray diffraction (XRD: M18XHF, Bruker AXS K.K.) patterns shown in Fig. 3 and 4, respectively. These allowed the thermal diffusivity (ai-Phase mobile 1, ai-Phase Co. Ltd.) and optical (FT/IR-700, Jasco Co. Ltd.) measurements on the freestanding YSZ coating.

The average thermal diffusivity of the YSZ coating was measured at room temperature by the Fourier transform thermal analysis at 15 different points of the coating (Ref 11). With the freestanding YSZ coating, apparent density was measured by the Archimedes method after the surface of the freestanding coating was covered with collodion films leaving the pores within the coating opened. Thermal conductivity of the coating was then estimated using the specific heat of YSZ (ZrO_2) (Ref 12, 13). The optical properties such as reflectance and transmittance were measured by Fourier transform infrared (FT-IR) spectrometer equipped with both integrating sphere detector and the microscopic mode.

Figure 5 shows the typical temperature profile measured at the back of the graphite substrate during the deposition experiment. It is seen clearly that the

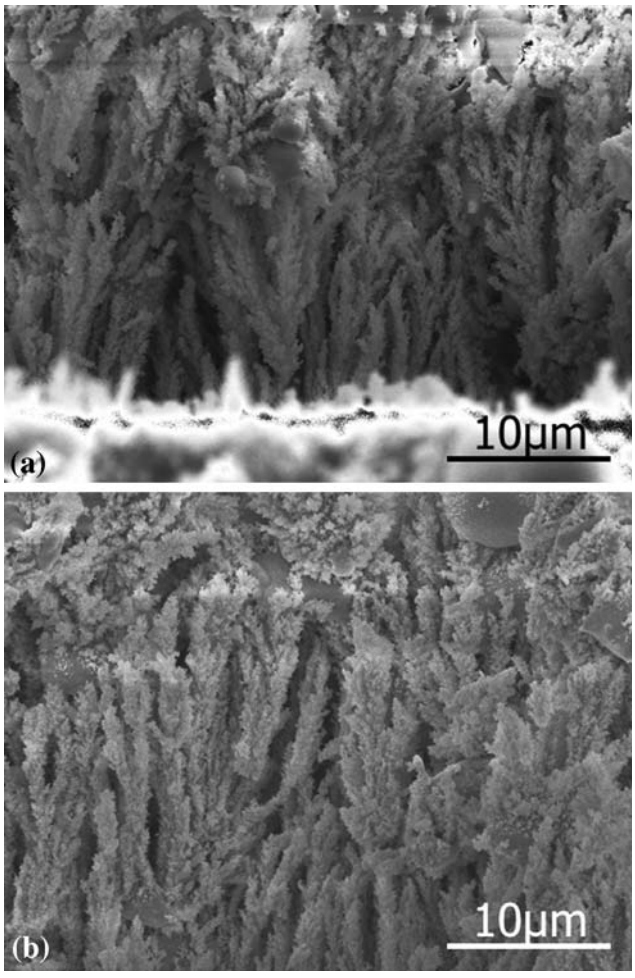

Fig. 3 Typical SEM cross-sectional image of the YSZ coating (a) before and (b) after 1200 °C annealing for 14 h. This specimen was deposited at 50 mm torch-to-substrate distance, on a 10 rpm revolution (other parameters are shown in Table 1)

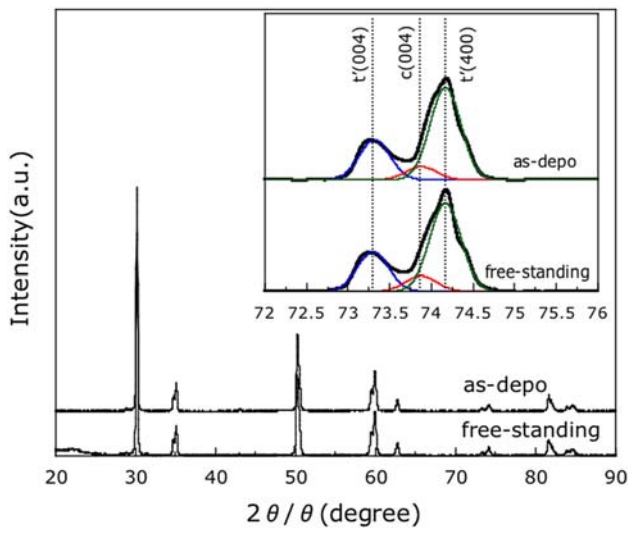

Fig. 4 Comparison of XRD patterns of the YSZ coating before (as-deposited) and after (free-standing) 1200 °C annealing for 14 h in ambient air

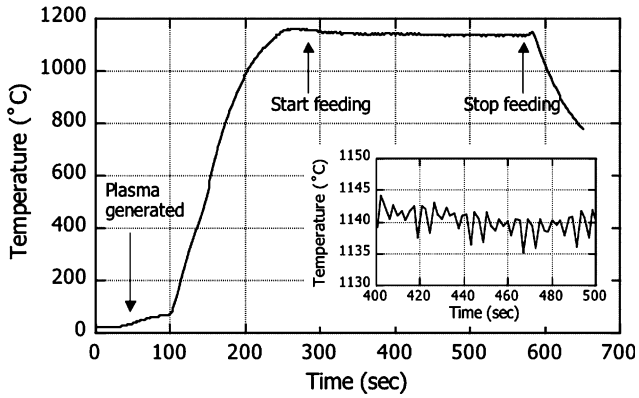

Fig. 5 Typical substrate temperature profile of the plasma spraying deposition process. The system enables the real-time temperature monitoring of the graphite substrate at its backside by R-type thermocouple during revolution. Inset shows the temperature fluctuation which roughly matches the frequency of the plasma flame exposure due to the substrate revolution

temperature increases significantly initially but saturates around 1140 °C, nearly 300 s after the plasma ignition. Accordingly, the powder injection was started when the temperature reached the constant value. Although the substrate was exposed to two plasma flames cyclically, the temperature fluctuates only within 10 °C range, as shown in the inset. The average temperature was found not to be affected much by the feeding rate or the substrate revolution speed (it can be reduced significantly by employing the effective water-cooled system). Therefore, the depositions in this work were carried out at ~1140 °C, unless otherwise stated.

3. Results and Discussion

3.1 Variation of Coating Microstructure

3.1.1 Effect of Powder Feeding Rates. The deposition rate was found to increase linearly with the feeding rate and the net deposition rate (the film thickness divided by the cumulative plasma exposure time for the actual deposition) reaches 100 μm/min at 0.8 g/min, 200 μm/min at 1.6 g/min, and 430 μm/min at 3.2 g/min. The cross-sectional SEM images of these YSZ coatings are shown in Fig. 6. The structures exhibit fundamentally porous structure irrespective of the feeding rates. However, the detailed structure was changed with the feeding rate. A feather-like structure with hefty branches (Fig. 6a) was deposited at low feeding rate of 0.8 g/min, and it changes to slimmer feather (Fig. 6b) at 1.6 g/min. This difference may be qualitatively explained by the change in the growth itself with feeding rate. The porous structures are formed fundamentally by the shadowing effect as a result of the substrate rotation. Therefore, when the feeding rate increases, the growth in the vertical direction becomes significant predominantly, as is evidenced by the increased in the deposition rate. This, however, causes further the

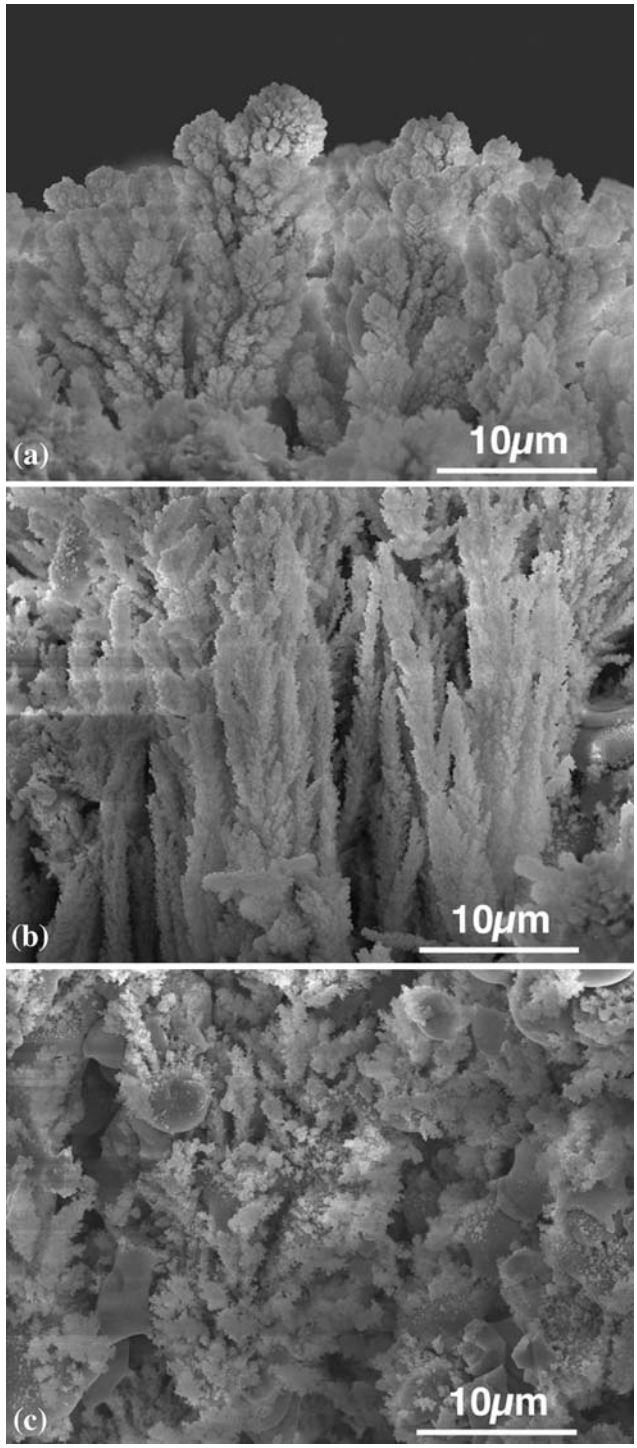

Fig. 6 Structural variation with feeding rates. (a) 0.8 g/min, (b) 1.6 g/min, and (c) 3.2 g/min (substrate revolution: 10 rpm)

shadowing effect and prevents the vapors from penetration between the branches, which eventually leads to slimmer structures at high feeding rate. With further increase in the feeding rate, however, although the majority of the structure still exhibits the vapor phase deposited structure, the solidified dense spherical grains were

observed from place-to-place possibly due to reduced heating efficiency to each particle as a result of loading (Fig. 6c). This clearly indicates that the feed rate of 3.2 g/min is too large to evaporate completely all the powders within the plasma and some powders were in the molten state in the plasma.

If one compares the structure (Fig. 6b) with that attained by a single torch under the same deposition condition shown in Fig. 2(b), no significant difference was observed. However, the coating deposited by twin torch system has shown stronger behavior against the physical contact in handling, although the degree of the macroscopic strength has not yet quantified. Therefore, these may suggest that the instantaneous exposure by the secondary plasma flame during deposition could be useful as far as it was not so significant to alter the porous structure.

3.1.2 Effect of Substrate Revolution Speed. In order to avoid the inclusion of solidified particles to the PVD structure while maintaining reasonably higher deposition speed, the feeding rate of 1.6 g/min was selected under the present plasma condition. Figure 7 compares the structures of the coatings deposited at different substrate revolution speed. It is seen that the structure exhibits fundamentally porous feather-like structure growing rather vertically to the substrate surface. Even if the revolution speed was increased by five times from 10 to 50 rpm, no significant change in the structure was observed. It was also found that the deposition rate was not affected by the revolution speed. The temperature of the substrate was also unchanged even if the substrate was moved quickly.

From the result of the plasma flow simulation with the code from Simulent Inc. (Toronto, Canada) under the present condition, the gas velocity at the hybrid torch exit was calculated to be in the range of 50 to 200 m/s. Taking account of the expansion after the torch exit, the gas flow in front of the substrate surface was estimated roughly to be at least several m/s. In contrast, the angular velocity of the substrate at the revolution speed of 10 to 50 rpm is 0.1 to 0.5 m/s. That is, the substrate speed in the transverse direction is at least one order smaller than the vapor velocity impinging on the substrate surface. Therefore, this may qualitatively explain the less significant effect of the revolution speed on the deposition process.

3.1.3 Effect of Coating Thickness. At a fixed feeding rate of 1.6 g/min and revolution speed of 10 rpm, the deposition time was prolonged to attain thicker coatings. The deposition rate was found to increase linearly with time, which corresponds to the net deposition rate of 200 μm/min. Figure 8 shows the cross-sectional SEM images of the coatings deposited for (a) 10 min and (b) 15 min. Compared to the structure deposited for a short time of 5 min (Fig. 7a), the structure seems to become denser especially at the surface of the coating.

In a separate experiment, a water-cooled copper substrate holder, where the water flow rate can be controlled, was mounted on a revolution holder, and the temperatures at the water inlet/outlet and at several positions within the copper holder were monitored during deposition. The averaged heat flux transferred to the substrate was estimated accordingly to be 4 MW/m^2 under the present plasma condition. The actual substrate temperature was somewhat constant at 1140 °C during deposition as shown in Fig. 5. Therefore, suppose that the porous YSZ coating with thermal conductivity <0.5 W/mK is continuously deposited on a graphite substrate with thermal

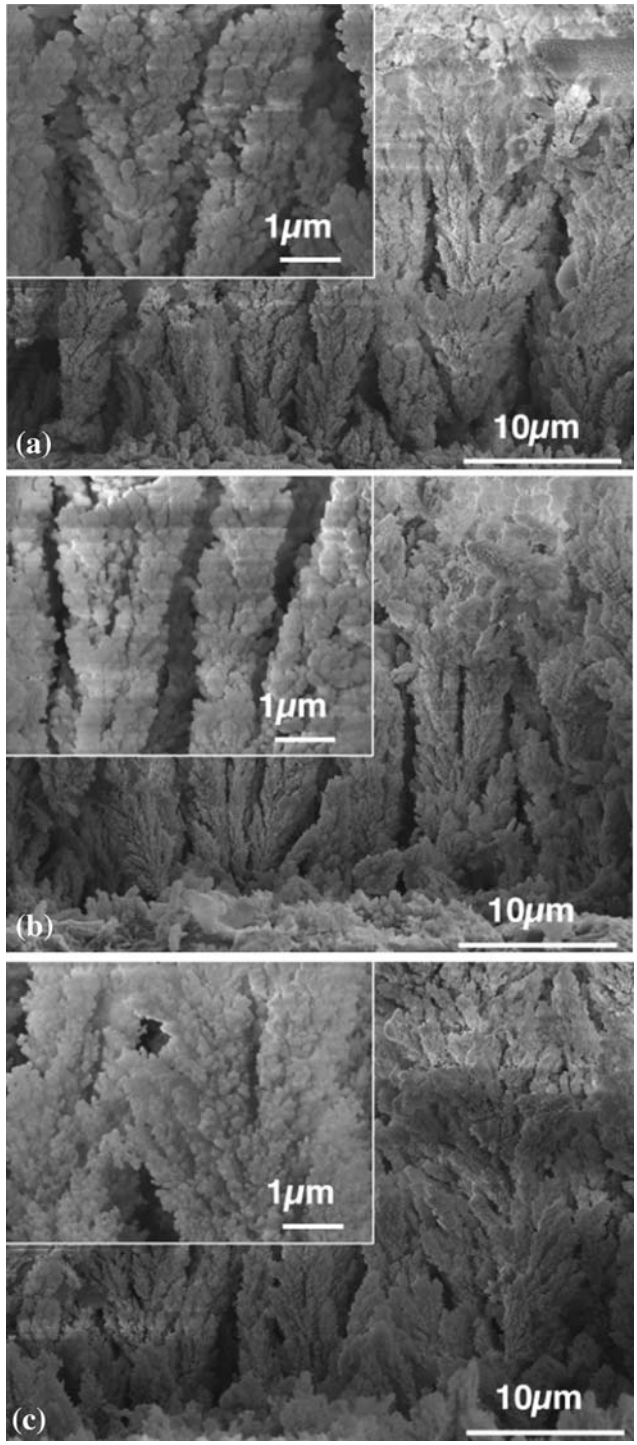

Fig. 7 YSZ cross-sectional structures deposited at different substrate revolution speeds: (a) 10, (b) 30, and (c) 50 rpm

conductivity of 170 W/mK at the constant backside temperature of 1140 °C, the topmost surface of the growing YSZ surface is roughly estimated to reach 2340 °C in 15 min which is nearly 86% of the YSZ melting point. Therefore, the surface temperature could increase momentarily and cause the excessive densification/melting at the fine feather tips of such a structure. Nevertheless, uniform porous coating structures can be deposited if the secondary plasma heating is to be controlled actively with the growth progress.

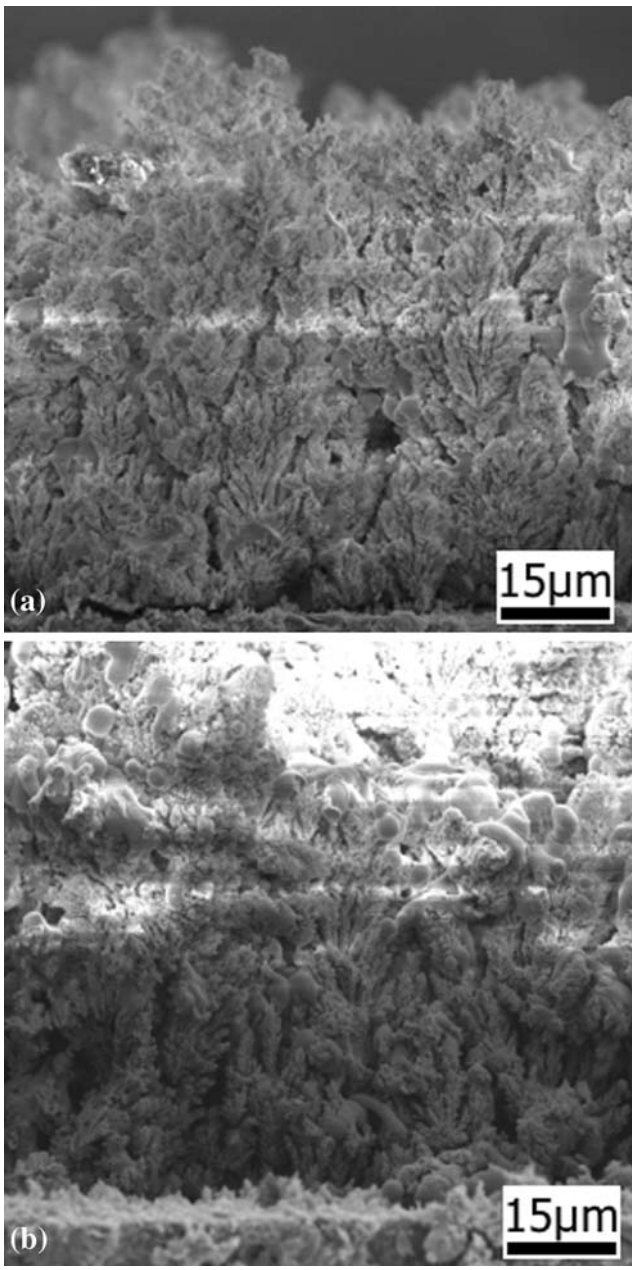

Fig. 8 Structure of the thicker YSZ coating: (a) 80 μm for 10 min and (b) 120 μm thick for 15 min deposition

3.2 Thermal and Optical Properties

The porosity and thermal conductivities of the coatings with different thickness are summarized in Fig. 9. It is noted that the porosity fundamentally reaches around 60% and the resultant thermal conductivity was significantly lowered to less than 0.5 W/mK. Although the structure of the thicker coating looks a little bit denser locally near the surface, it still attains low thermal conductivity compared to that generally attained by APS and EB-PVD (Ref 2, 3).

Since YSZ is transparent to infrared (IR), upon being employed as TBCs at elevated temperature, the IR reflection capability incorporated by the structure has to be considered to prevent radiative heating of the underlying substrate. Figures 10 and 11 show the transmittance and reflectance of the PS-PVD YSZ coatings, deposited at 1.6 g/min, 10 rpm (these structures are shown in Fig. 7a, 8). It is seen that the reflectance of the thick PS-PVD YSZ coating reaches nearly 70% in the 2 to 6 μm range, which is much larger than that attained by the PPS coating. As a result, the transmittance is reduced significantly to 20 to 30%. This contrasts to the value ~80% for the single crystal YSZ (280 μm thick), ~40% for the sprayed splat coatings by this system (120 μm thick), and 30-40% for APS with 170 μm thick (Ref 14, 15). The absorption (attenuation) is estimated accordingly to be 10% in a few μm wavelengths. In addition, if compared with the values measured by the microscopic mode, although the transmittance obtained by the integrating sphere is only slightly large, the reflectance is pronouncedly higher than that of the microscopic mode for all the specimens. These readily

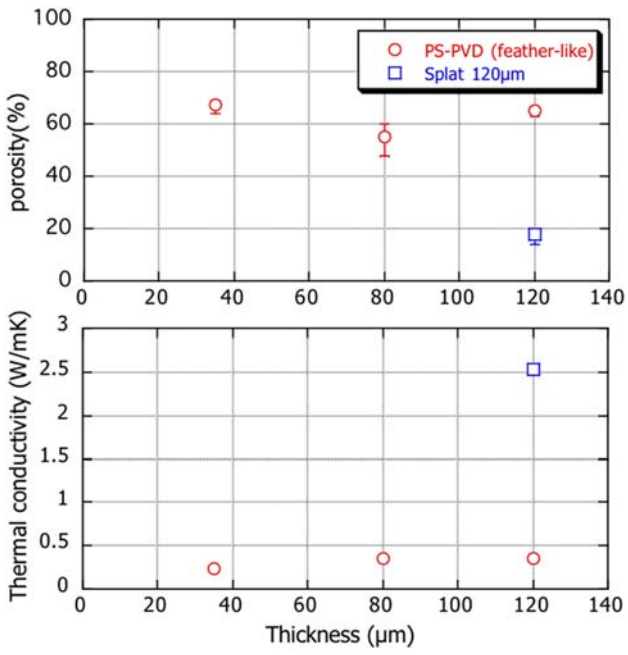

Fig. 9 Variation of porosity and thermal conductivity of the YSZ coatings with different thickness. Value of the sprayed splat coatings deposited by this system is compared

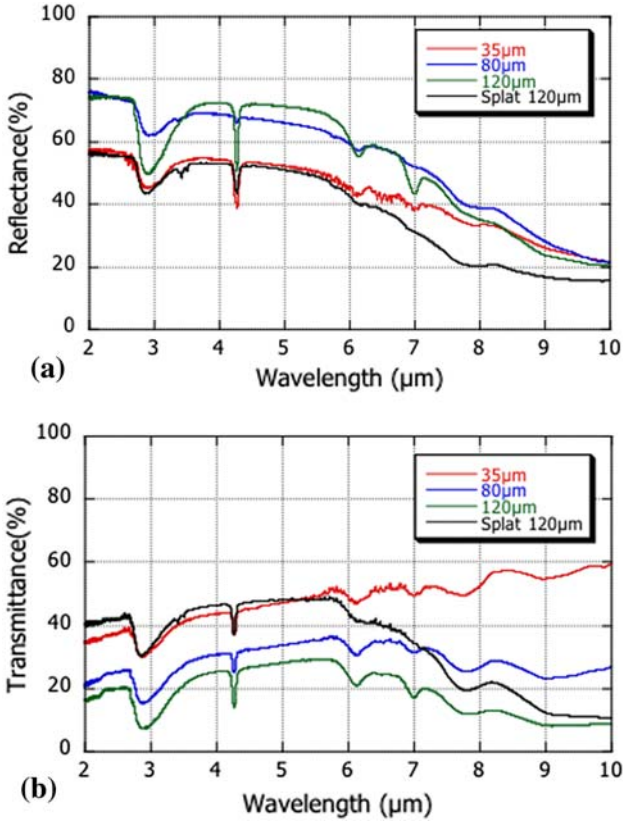

Fig. 10 FT-IR (a) reflectance and (b) transmittance of the YSZ PS-PVD measured by integrated sphere detector (10 mm diameter window). The error in the values measured at different positions was found less than 5%

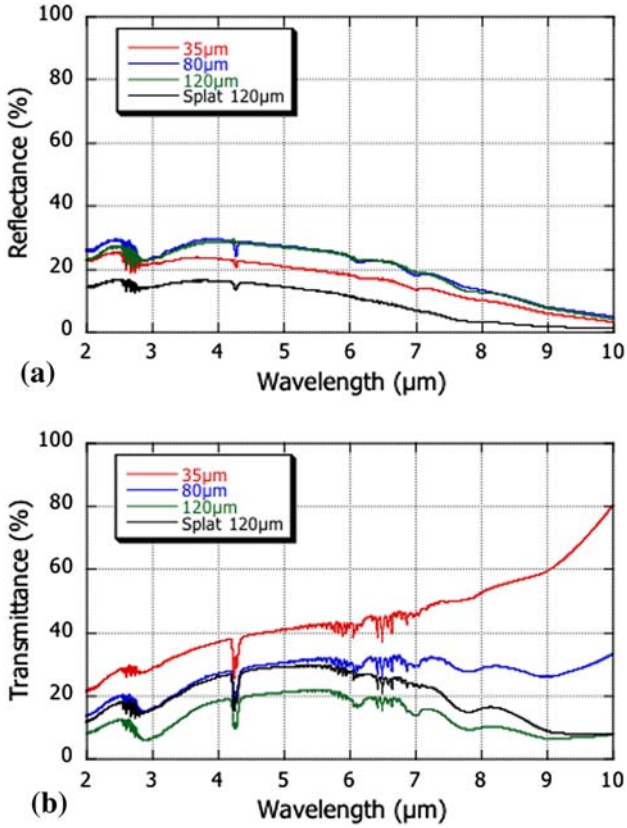

Fig. 11 FT-IR transmittance (a) and reflectance (b) of the PS-PVD YSZ coatings with different thickness, measured by the 10-μm diameter beam microscopic measurement mode with a 40° conical lens

confirm the diffuse (random) scattering nature of both sprayed splat and feather-like structures, and also indicate more significant IR scattering by the feather-like structure. Effects of the thickness and surface morphology of this structure are, however, not clearly seen in the present measurement, as the thin YSZ (35 μm) coating may be so porous as to allow the light penetration locally. Nevertheless, these results underline the effective IR shield capability of the PS-PVD structure.

4. Conclusions

Feather-like porous YSZ coatings have been deposited by plasma spray PVD at the deposition rate of 220 μm/min. In-process annealing was found effective to attain free-standing coatings, without deteriorating the unique nano-structure. Such a porous YSZ has exhibited room temperature thermal conductivity of less 0.5 W/mK and high effective IR reflectance, both of which characterize this coating as unique TBCs. As mentioned in the introduction section, we have demonstrated high dense t′ YSZ coatings by the plasma spray PVD (Ref 9). Therefore, these feather-like structure coatings can be integrated as a middle layer of a novel multi functional three-layered top coat, composed of large grained splat layer at the bottom and high dense and hard layer at the top, by a simple modification of the plasma spray PVD condition with the identical facility.

References

1. X. Cao, R. Vassen, and D. Stoever, Ceramic Materials for Thermal Barrier Coatings, *J. Eur. Ceram. Soc.*, 2004, **24**(1), p 1-10
2. H.B. Guo, R. Vasen, and D. Stover, Thermophysical Properties and Thermal Cycling Behavior of Plasma Sprayed Thick Thermal Barrier Coatings, *Surf. Coat. Technol.*, 2005, **192**, p 48-56
3. J.R. Nicholsa, K.J. Lawsona, A. Johnstoneb, and D.S. Rickerbyb, Methods to Reduce the Thermal Conductivity of EB-PVD TBCs, *Surf. Coat. Technol.*, 2002, **151-152**, p 383-391
4. P. Proulx, J. Mostaghimi, and M.I. Boulos, Plasma-Particle Interaction Effects in Induction Plasma Modeling Under Dense Loading Conditions, *Int. J. Heat Mass Transfer*, 1985, **28**, p 1327-1336
5. R. Ye, P. Proulx, and M.I. Boulos, Particle Turbulent Dispersion and Loading Effects in an Inductively Coupled Radio Frequency Plasma, *J. Phys. D: Appl. Phys.*, 2000, **33**, p 2154-2162
6. M. Kambara, A. Shinozawa, K. Aoshika, K. Eguchi, and T. Yoshida, Development of Porous YSZ Coatings with Modified Thermal and Optical Properties by Plasma Spray Physical Vapor Deposition, 2009, submitted
7. K. Eguchi, H. Hej, M. Kambara, and T. Yoshida, Twin Hybrid Plasma Spray Deposition of Novel Thermal Barrier YSZ Composite Coatings, *J. Jpn. Inst. Metals*, 2005, **69**, p 17-22

8. H. Heji, K. Eguchi, M. Kambara, and T. Yoshida, Ultrafast Thermal Plasma Physical Vapor Deposition of Yttria-stabilized Zirconia for Novel Thermal Barrier Coatings, *J. Therm. Spray Technol.*, 2006, **15**, p 83-91
9. J. Li, H. Huang, T. Ma, K. Eguchi, and T. Yoshida, Twin-structured Yttria-stabilized t' Zirconia Coatings Deposited by Plasma Spray Vapor Deposition: Microstructure and Mechanical Properties, *J. Am. Ceram. Soc.*, 2007, **90**, p 603-607
10. T. Yoshida, T. Tani, H. Nishimura, and K. Akashi, Characterization of a Hybrid Plasma and its Application to a Chemical Synthesis, *J. Appl. Phys.*, 1983, **54**, p 640-646
11. J. Morikawa and T. Hashimoto, New Technique for Fourier Transform Thermal Analysis, *J. Therm. Anal. Calorim.*, 2001, **64**(1), p 403-412
12. B.-K. Jang and H. Matsubara, Thermophysical Properties of EB-PVD Coatings and Sintered Ceramics of 4 mol% Y2O3-Stabilized Zirconia, *J. Alloys Compd.*, 2006, **419**, p 243-246
13. http://webbook.nist.gov/chemistry/form-ser.html
14. J.I. Eldrige, C.M. Spucker, and R.E. Martin, Monitoring Delamination Progression in Thermal Barrier Coatings by Mid-Infrared Reflectance Imaging, *Int. J. Appl. Ceram. Technol.*, 2006, **3**, p 94-104
15. J.I. Eldridge, C.M. Spuckler, K.W. Street, and J.R. Harkham, Infrared Radiative Properties of Yttria-Stabilized Zirconia Thermal Barrier Coatings, *Ceram. Eng. Sci. Proc.*, 2002, **23**, *The 26th Annual International Conference on Advanced Ceramics & Composites*, Florida, U.S.A., p 417-430